2021-01-0069 Published 06 Apr 2021

Using Demanded Power and RDE Aggressiveness Metrics to Analyze the Impact of CACC Aggressiveness on Heavy Duty Platooning Power Consumption

Jan Siefert, Evan Stegner, Philip Snitzer, Jacob Ward, David M. Bevly, and Mark Hoffman Auburn University

Andrew Kotz National Renewable Energy Laboratory

Citation: Siefert, J., Stegner, E., Snitzer, P., Ward, J. et al., "Using Demanded Power and RDE Aggressiveness Metrics to Analyze the Impact of CACC Aggressiveness on Heavy Duty Platooning Power Consumption," SAE Technical Paper 2021-01-0069, 2021, doi:10.4271/2021-01-0069.

Abstract

Presently, a main mobility sector objective is to reduce its impact on the global greenhouse gas emissions. While there are many techniques being explored, a promising approach to improve fuel economy is to reduce the required energy by using slipstream effects.

This study analyzes the demanded engine power and mechanical energy used by heavy-duty trucks during platooning and non-platooning operation to determine the aerodynamic benefits of the slipstream. A series of platooning tests utilizing class 8 semi-trucks platooning via Cooperative Adaptive Cruise Control (CACC) are performed. Comparing the demanded engine power and mechanical energy used reveals the benefits of platooning on the aerodynamic drag while disregarding any potential negative side effects on the engine.

However, energy savings were lower than expected in some cases. It was hypothesized that the CACC may have amplified transient platooning events relative to the individual truck baseline results, hampering the potential energy savings. Therefore, the impact of the controller on the observed driving style was analyzed in detail. In order to quantify the transient operational characteristics of the experimental trials, metrics from the European Real Driving Emissions (RDE) legislation were modified to serve as metrics of aggressiveness during platooning.

The metrics $(v \cdot a_{pos})^{95}$ and Relative Positive Acceleration (RPA) were calculated for platooning and non-platooning runs. These results indicate that the CACC induces small acceleration events during platooning to retain the commanded longitudinal separation between vehicles. These small acceleration events increase following vehicle aggressiveness during platooning and prevent the following vehicles from obtaining maximum energy savings.

Moreover, a correlation between the RDE metric $(v \cdot a_{pos})^{95}$ and energy savings is developed. Hence, this work establishes the ability of RDE metrics to assess CACC impacts on platoon energy savings.

Introduction and Motivation

Heavy duty and passenger car sectors are emphasizing reduced energy consumption. While this can be done by improving existing powertrains or using alternative drive systems, it can also be achieved by reducing the overall resistance to vehicle motion. The latter is mainly driven by rolling resistance and aerodynamic drag [1]. A reduction in either of those resistances increases the efficiency of any vehicle regardless of its drive system. This possibility of improving transportation independently from the drive systems highlights the significance of this objective.

Despite the fact that light duty transportation is responsible for the majority of traffic, heavy duty transportation is still responsible for 23% of the total USA transportation sector greenhouse gas emissions [2]. In contrast to passenger cars fuel costs are the number two expense next to wages in the heavy duty sector, placing increased emphasis on energy savings through return on investment metrics [3].

While rolling resistance is mainly a function of powertrain losses and tire-pavement interaction, the largest short-term improvements are expected for reducing aerodynamic drag. One promising approach is utilizing automated driving technologies that enable groups of vehicles to act together toward energy savings. A possible utilization for these technologies is platooning, where a group of vehicles is traveling at longitudinal spacings small enough to realize aerodynamic energy consumption benefits. During platooning, aerodynamic effects lead to a drag reduction. The quantity of drag reduction is dependent on the vehicle position within the platoon. The benefit for trailing vehicles is considered significantly higher than for leading vehicles [4]. However, due to an increased draft pressure or "push" leading vehicles also experience net energy savings for close following distances.

Although human drivers are capable of platooning manually, only a computer can safely follow at distances less than 100 m, where platooning is most energy effective [5]. Since the highest aerodynamic benefits are realized at close following distances, the vehicle's longitudinal controller must be safely tuned. With safety as the highest-ranking objective, a controller has to be also tuned to allow the highest energy savings possible. These two control tasks can be in competition.

Headway platooning controllers can induce oscillations in the following trucks, resulting in transient events where following trucks try to either catch up or fall back. Imposition of additional transiency may reduce energy savings during platooning. This transiency is especially problematic for heterogeneous platoons composed of different trucks and control systems, and for platoons subject to disturbances such as heavy grades or cut-ins. In the vast majority of prior studies, platooning performance has been assessed in terms of either fuel savings [5, 6] or control performance [7], but not both. Because of the aforementioned influence of controls on platoon fuel efficiency, methodologies that describe the relationship between the two factors will be critical to optimize platoon operation.

The first step toward linking platooning control performance with fuel performance is the development of metrics comparing the controller's influence on the trip dynamics. In this analysis, metrics from the European Real Driving Emissions (RDE) regulations were adapted for this purpose. RDE metrics were designed to measure the driver-induced aggressiveness on real world passenger car driving. The RDE metrics were designed to possess a directly proportional relationship with driver induced dynamics [8]. In this investigation, platoons attempt to maintain a constant speed paced by the lead truck. RDE analysis of each platoon follower relative to baseline operation as a solo vehicle will elucidate the relationship between CACC operation and trip dynamics. The study herein shows that RDE metrics can be adopted to platooning and reveals that a correlation between these metrics and energy savings exists. Therefore, this study is one of the few studies that documents both energy savings and control performance.

Accurate fuel quantification requires research grade instrumentation unavailable for this investigation. Additionally, utilization of fuel measurements can complicate the analysis through potential disparities in the internal combustion engine thermal efficiency due to platooning conditions. Namely, these efficiency disparities may be caused by a change in intake air mass or change in intake air temperature due to platooning [9]. Therefore, this study utilizes engine torque and engine speed to calculate the engine power and eventually the mechanical energy used at the crankshaft. This allows isolation of the actual reduced aerodynamic drag impacts without becoming blurred by possible engine efficiency alterations.

After describing the trucks used in the experiment, their platooning control system and the test conditions, a broad overview about the data processing will be presented. Accordingly, the RDE metrics will be introduced and discussed. Then, the results are presented, followed by a summary of the findings, and avenues for future investigation.

Experimental Methods

Trucks and Control System

In total, four trucks were used for this study. A 2015 Peterbilt 579 with a Paccar engine (A1), a 2015 Peterbilt 579 with a Cummins engine (A2), an unarmored 2009 Freightliner M915A5 with a Detroit Diesel engine (T14), and an armored 2009 Freightliner M915A5 with a Detroit Diesel engine (T13). All attached trailers were of the dry-van type and unloaded. Detailed specifications can be found in Table 1.

To ensure robust on-road platooning performance, the Coordinated or Cooperative Adaptive Cruise Control (CACC) being developed by the GPS and Vehicle Dynamics Laboratory (GAVLAB) at Auburn University is utilized in this study. The CACC system includes a Dedicated Short Range Communications (DSRC) radio allowing Vehicle to Vehicle (V2V) communication. Furthermore, GPS, radar and wheel-speed measurements are applied within the range estimator. The CACC system interfaces to the trucks via their Controller Area Networks (CAN) and utilizes the existing Adaptive Cruise Control (ACC) architecture to command the throttle and braking systems. The control and estimation algorithms run on a standalone computer using a Robot Operating System (ROS). Even though the trucks are equipped with electrically assisted steering wheels, the trucks were manually steered in this testing campaign. More details on the used CACC can be found in previous publications [7, 10, 11, 12, 13].

Test Tracks

This study utilizes data collected on two different test tracks: the 2.73 km-long National Center for Asphalt Technology (NCAT) oval test track in Opelika, Alabama (see Figure 1), and the 3.7 km-long American Center for Mobility (ACM) test track in Ypsilanti, Michigan (see Figure 2).

Physical differences between the two tracks creates a broad spectrum of road conditions, inducing a wide range of dynamics. Namely, the grade at NCAT is almost negligible

TABLE 1 Specifications of the trucks

Truck ID	A1	A2	T14	T13
Manufacturer	Peterbilt	Peterbilt	Freightliner	Freightliner
Model	579	579	M915A5	M915A5
Model Year	2015	2015	2009	2009
Engine	Paccar MX-13	Cummins ISX15-415ST2	Detroit Diesel IV S60	Detroit Diesel IV S60
Peak Torque	2372 Nm	2237 Nm	2237 Nm	2237 Nm
Rated Horsepower	430 bhp	415 bhp	500 bhp	500 bhp
Truck & Trailer Gross Weight	16175 kg	17245 kg	17234 kg	21295 kg

FIGURE 1 Overview of the NCAT test track

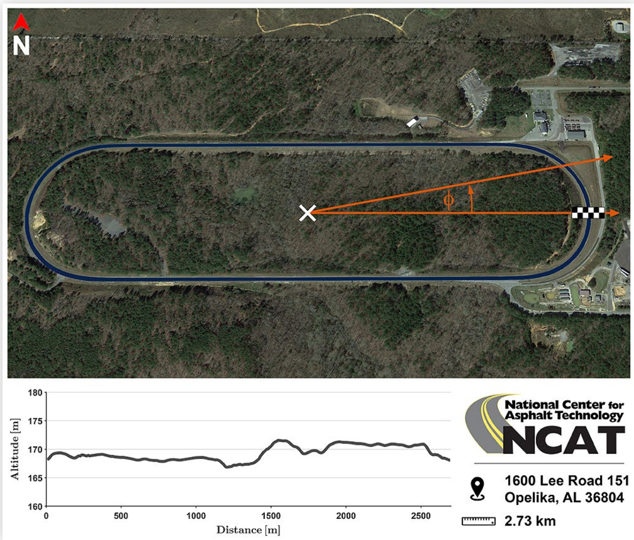

FIGURE 2 Overview of the ACM test track

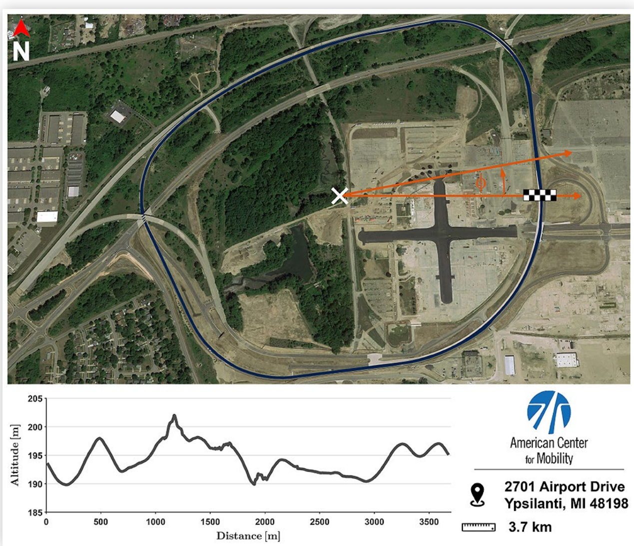

while ACM contains a more demanding grade profile. Therefore, using data from both test tracks increases the representativeness of actual on-road driving. The weather at both locations during the test campaign is described in Table 2 and Table 3 in the Appendix.

Test Procedure

A test matrix was designed to accentuate the impacts of truck heterogeneity on platooning performance (see Figure 3). The three distinct platoon configurations were then tested at different headway distances: 100 ft (30.48 m), 50 ft (15.24 m) and 35 ft (10.67 m). Baseline, or standalone, operation of each individual vehicle was used to establish the relative platooning benefits.

Before starting the test runs, the trucks were actively conditioned by warming them up for 1 h on-road. Furthermore, the downtime between tests was kept at 30 min. Performing this routine prior to every test minimizes changes in parameters like tire pressure and temperature, engine coolant temperature, etc.. During testing, engine fans were manually turned on to ensure consistency between baseline and platooning runs. In addition to that, active regeneration of the diesel particulate filters was disabled. The speed for a test run was set to 45 mph ($72.4\,\frac{\text{km}}{\text{h}}$) on both tracks. One test was set up for roughly 1 h, which resulted in 26 laps at NCAT and 19 at ACM. Several of those test runs were performed for each platooning configuration. The CAN data utilized in this study was recorded at 1 Hz.

Data Processing

One aim of this study was to examine the dynamics and energy consumption on a per lap basis. Therefore, data had to be sectioned into laps. This has been done by approximating the center of each track (see white crosses in Figures 1 and 2) and by calculating the polar coordinates of the truck's GPS-based track position at every second. The virtual start-finish line, designated $\Phi = 0\,°$, was set to the east of the center of track. Once Φ reaches 360°, one lap has been completed and the data was stored in a separate structure allowing a lap-wise analysis. Using Φ to define the position leads to distortions for any non-circular track. Therefore, the wheel speed signal was integrated to determine the distance traveled per lap.

Analyzing results on a lap basis requires a quality control to ensure all laps are comparable. Different approaches exist for lap evaluation. For example, using CAN fuel rate [10], using recorded headway, or using speed signal to find runaway laps. This study focuses on the raw benefits of platooning on driving resistance, therefore the speed signal was used to characterize the quality of a lap. Figure 4 shows lap-wise speed traces for T14 while operating in a two-truck platoon with a 50 ft headway. In Figure 5 all the self-similar laps for truck T14 at ACM are shown as scatters with their moving average as a solid line. This comparison shows, that there is a characteristic speed trace for each platooning configuration, and that using the speed signal for lap evaluation does result in comparable laps.

FIGURE 3 Platoon configurations tested

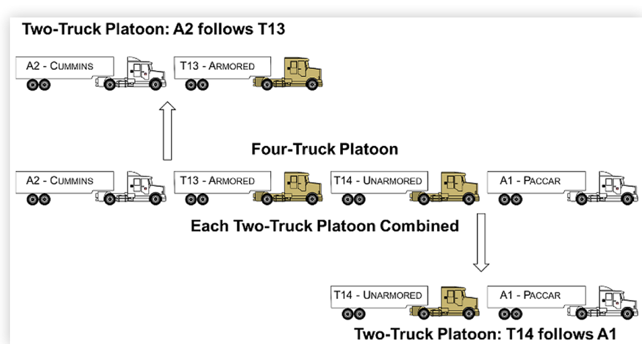

FIGURE 4 Speed traces of all T14 50 ft two-truck laps at ACM and during lap evaluation determined self-similar indicative laps

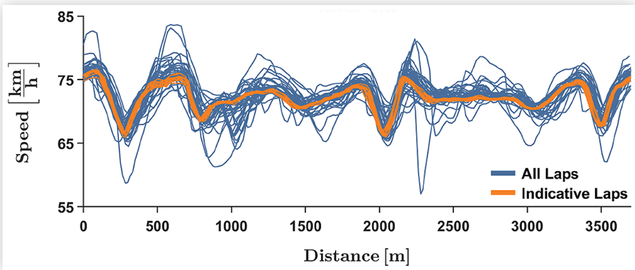

FIGURE 5 Speed traces of all self-similar indicative laps and their moving averages for all platoon configurations of T14 at ACM

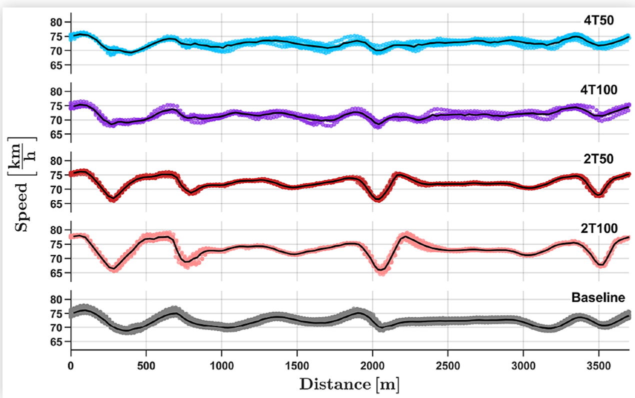

For all the indicative laps, the engine power and total mechanical energy usage was then calculated as stated in the Equations 1 to 3.

$$T_{Engine,i} = \frac{T_{Peak} \cdot T_{Actual,\%}}{100} \quad (1)$$

$$P_{Engine,i} = 2 \cdot \pi \cdot T_{Engine,i} \cdot n_{Engine,i} \cdot 1000 \quad (2)$$

$$P_{Consump.,Lap} = \frac{\sum_i P_{Engine,i} \cdot \Delta t}{3600} \quad i = 1 \ to \ K \quad (3)$$

with: i = Time step

T_{Peak} = Engine peak torque (see Table 1) [Nm]

$T_{Engine,\,i}$ = Engine torque at time step i [Nm]

$T_{Actual,\,\%}$ = Engine percent torque at time step i [%]

$P_{Engine,\,i}$ = Engine power at time step i [kW]

$n_{Engine,\,i}$ = Engine rpm at time step i $\left[\frac{1}{s}\right]$

$P_{Consump.,\,Lap}$ = Mechanical energy used per lap [kWh]

K = Number of time steps per lap

Δt = Duration between time steps [s]

RDE Metrics

The Commission Regulation (EU) 2017/1151 describes the implementation of real world testing into the type-approval of motor vehicles in the European Union [14]. Testing Real Driving Emissions (RDE) on public roads takes away the repeatability and comparability of the previous laboratory-based cycle testing. Therefore, new metrics and boundary conditions were established to ensure high repeatability and comparability of RDE test runs.

A variable with huge impact on the RDE test results are the drivers and the dynamics they induce to the vehicle. To take away a driver's influence on the RDE test run, the metrics $(v \cdot a_{pos})^{95}$ and Relative Positive Acceleration *RPA* were introduced to verify the overall trip dynamics. This study attempts to use these metrics to describe the dynamics induced by the adaptive cruise controllers and find a correlation between the RDE metrics and energy savings during platooning. Detailed steps to calculate these metrics can be found in Appendix 7a "Verification of overall trip dynamics" in the Commission Regulation (EU) 2017/1151. Subsequently, only the most important steps are shown. Aside from that, a brief summary of all the steps is shown in Figure 6.

The calculations' only input is a time discretized speed signal at a sampling frequency of 1 Hz. The speed signal must match certain criteria to be considered sufficiently accurate. One criteria being determined through calculation of the acceleration resolution $a_{res.}$. If $a_{res.} \leq 0.01 \frac{m}{s^2}$ the speed signal is considered sufficiently accurate. The acceleration resolution was calculated for each truck and each run on both test tracks. The worst acceleration resolution found was $0.00108 \frac{m}{s^2}$ (see Figure 7). Therefore, the input signals were considered accurate enough and no filtering was necessary.

After calculating the acceleration a_i in every time step, the product $(v \cdot a)_i$ is then calculated. Since the focus of these RDE metrics is purely on acceleration events, a threshold was defined to differentiate between acceleration and deceleration. In Commission Regulation (EU) 2017/1151, the threshold is defined as $a_{pos.} = a\left(a > 0.1 \frac{m}{s^2}\right)$. Diverting these metrics from their intended use for real driving of passenger cars to constant speed platooning on a lap basis demands an adaptation of that threshold. This study has found, that a threshold of

FIGURE 6 Step by step calculations of RDE dynamic metrics

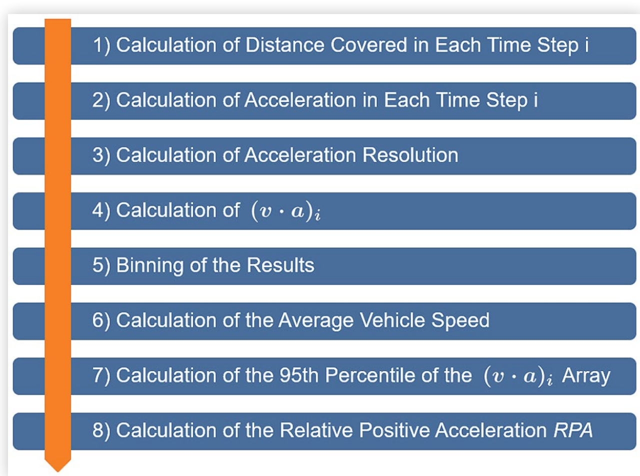

FIGURE 7 Calculated acceleration resolutions for all trucks and test runs

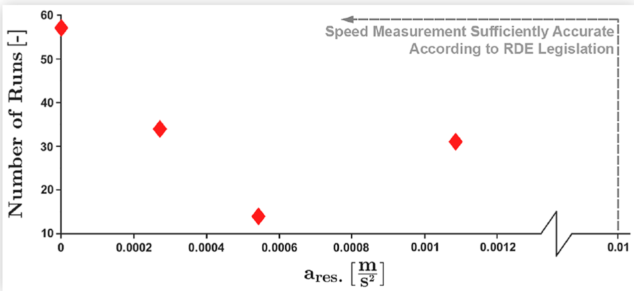

$a_{pos.} = a\left(a > 0.03\frac{\text{m}}{\text{s}^2}\right)$ leads to acceptable results for this testing campaign. The chosen threshold is approximately 30 times higher than the worst acceleration resolution measured during the testing campaign. In contrast, the RDE threshold for positive acceleration is only 10 times higher than the worst acceptable acceleration resolution. Data provided by future studies will help determine an acceptable threshold for platooning with near constant speed profiles. For lap-wise testing and comparison of results, a higher threshold decreases the amount of data points per lap disproportionately. For continuous testing on highway or interstate, a threshold closer to the RDE recommendation might be feasible.

Eliminating all non-acceleration time stamps using the threshold leads to the new naming convention of $(v \cdot a_{pos})_i$. In contrast to the RDE regulations, a separation into urban, rural and motorway speed bins is not performed because the trucks do not change their speed significantly during platooning. Therefore, the calculations were adjusted to a single speed bin for all time steps. To calculate $(v \cdot a_{pos})^{95}$ the $(v \cdot a_{pos})_i$ array is sorted in ascending order and the 95th percentile of that array is found or interpolated linearly (see Figure 8 and 9). The Relative Positive Acceleration (RPA) is calculated as stated in Equation 4. The calculation of $(v \cdot a_{pos})^{95}$ and RPA is performed for every single lap. As a result, lap averages can be compared between baseline and platooning runs.

FIGURE 8 All $(v \cdot a_{pos})i$ arrays for truck A1 and their moving average at NCAT

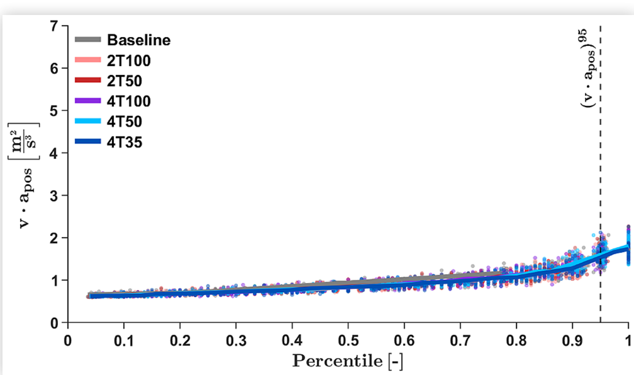

FIGURE 9 All $(v \cdot a_{pos})i$ arrays for truck A2 and their moving average at NCAT

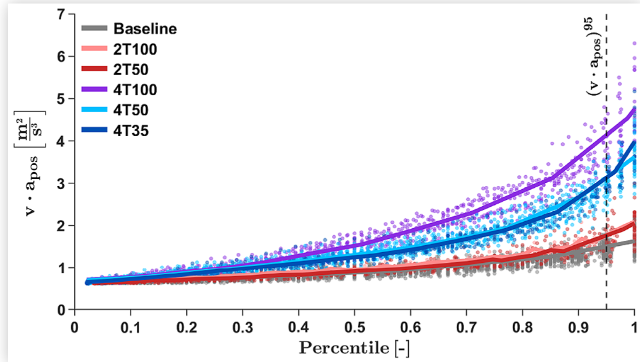

$$RPA = \frac{\sum_j (v \cdot a_{pos})_j}{\sum_i d_i} \quad j = 1 \ to \ M, \quad i = 1 \ to \ N \tag{4}$$

with M = Sample number with positive acceleration
N = Total number of samples
d_i = Distance covered in time step i [m]

In the RDE regulation, $(v \cdot a_{pos})^{95}$ is bound above and RPA bound below. However, both metrics increase with increasing driving dynamics. The thought experiment of a run with a perfectly constant speed trace helps understand the metrics. A constant speed trace has zero acceleration events. Therefore, the $(v \cdot a_{pos})_i$ array is empty. Hence, both $(v \cdot a_{pos})^{95}$ and RPA would trend to zero. The closer both metrics get to zero, the less transient the run was. The higher both metrics are, the more aggressive a run was. Therefore, both of them can be used to determine the influence of the controller on the transient behavior of the trucks during platooning.

Results and Discussion

$(v \cdot a_{pos})^{95}$ and RPA Results

The aim of this study was to apply RDE aggressiveness metrics to platooning and determine a correlation between the metrics and potential energy savings during platooning tactics. The two metrics available are $(v \cdot a_{pos})^{95}$ and RPA. To understand which metric is the most sensitive to aggressive maneuvers, data was collected for both variables during platooning and then compared to their respective baseline laps.

Figures 10 and 11 show this comparison for truck A2 at ACM's track. While the absolute values of $(v \cdot a_{pos})^{95}$ and RPA are different, their trends are very similar, which was observed for every truck, on both tracks. This suggests either metric can be used to assess platooning aggressiveness and correlation to energy savings. Moving forward, $(v \cdot a_{pos})^{95}$ will be used as the aggressiveness metric in this study.

FIGURE 10 *RPA* of all laps and their averages for A2 on ACM test track

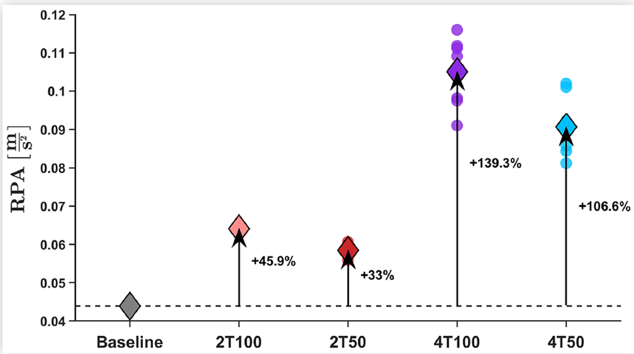

FIGURE 11 $(v \cdot a_{pos})^{95}$ of all laps and their averages for A2 on ACM test track

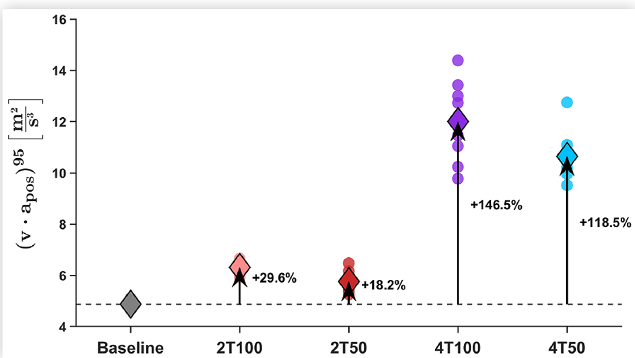

Power Demand and Energy Savings

While Figure 5 shows characteristic speed traces for different platooning configurations differ slightly from each other, the same was observed for the engine power throughout a lap.

Figure 12 shows the moving averages of all indicative laps for each platooning configuration of T13 at NCAT. In addition to the actual engine power, the grade of the track and the actual longitudinal acceleration are displayed. All moving averages show the engine is following the grade qualitatively. However, the shape of the two-truck and four-truck runs exhibit some significant differences, because T13 leads it two-truck platoons but is third in line during four-truck platoons. Clearly the controllers are amplifying dynamics when following another truck, which is directly passed down to engine power.

While the amplification is noticeable at NCAT, it is even more prominent during ACM testing (see Figure 13), where the grade profile forces the trucks to operate over a wider power and RPM spectrum (see Figure 14).

To see if increased following truck transiency has an impact on the platoon energy savings, all two-truck platooning results are compared in Figure 15. For this comparison, the total mechanical energy consumed for each lap was normalized with the average energy utilized during the baseline runs on the respective tracks. If the result of this normalization is a negative value, the total energy of the platooning lap was less than the individual truck's baseline operation. If the value is positive, there were either no aerodynamic benefits, or the increased transiency erased the possible energy savings.

FIGURE 12 Grade of the NCAT test track, and T13 longitudinal acceleration and engine power moving averages for the disparate platoon configurations at NCAT

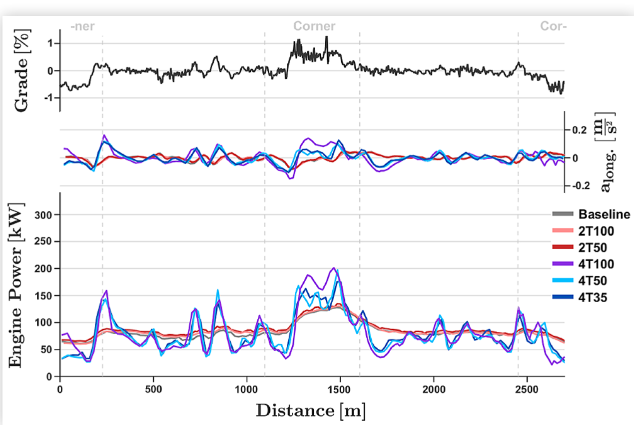

FIGURE 13 Grade of the ACM test track, and T13 longitudinal acceleration and engine power moving averages for the disparate platoon configurations at ACM

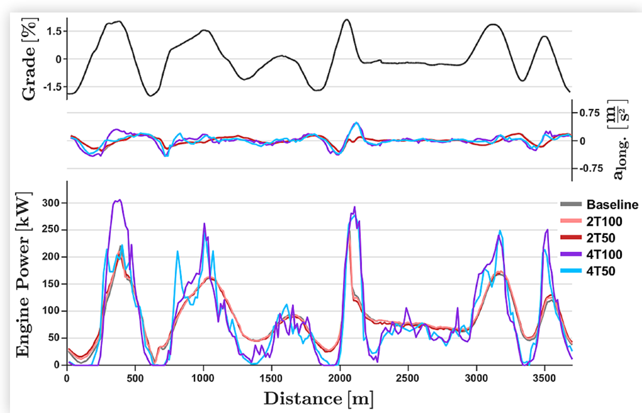

FIGURE 14 Engine power distribution for all baseline and platooning runs of T13 at ACM and NCAT

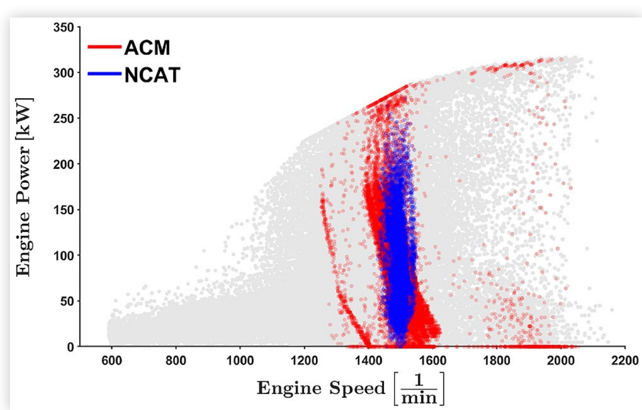

FIGURE 15 Overall energy savings per lap for the following trucks in two-truck platoons

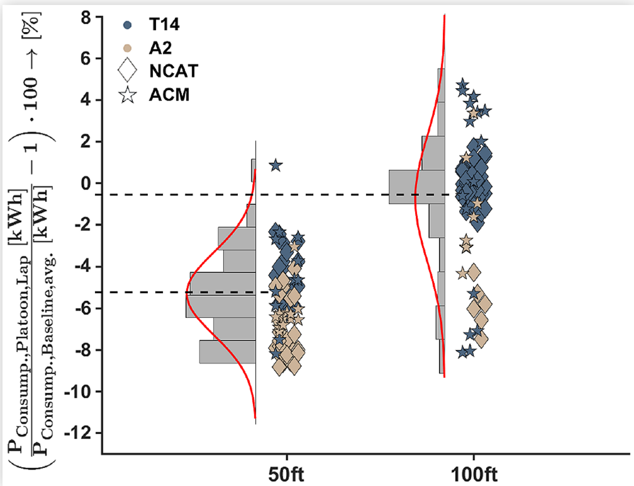

The calculated normalized distribution for followers at 50 ft shows a maximum energy saving of −5.2%. In contrast, followers at 100 ft receive only a small reduction of −0.5%.

Normalizing $(v \cdot a_{pos})^{95}$ in the same way indicates 100 ft runs were more transient than the 50 ft runs (see Figure 16). This implies that there might be a correlation between $(v \cdot a_{pos})^{95}$ and energy savings. In other words, the increased aggressiveness has washed away the aerodynamic benefits for the 100 ft runs.

Correlation between $(v \cdot a_{pos})^{95}$ and Energy Savings

To further investigate the correlation between measured aggressiveness and energy savings, four-truck platoons were analyzed as well. While trucks in four-truck platoons are exposed to pushing effects and reduced drag, a different approach was taken to make those correlations visible.

FIGURE 16 Overall change in $(v \cdot a_{pos})^{95}$ per lap for the following trucks in two-truck platoons

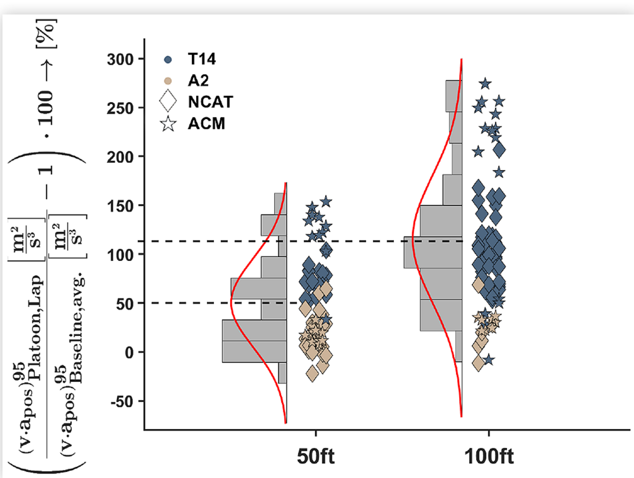

Figures 17 and 18 show the normalized average energy savings and aggressiveness for all four-truck, 100 ft headway operation on each test track. Numbers greater than zero represent increased aggressiveness and an increased energy use compared to the baseline runs while negative values show the opposite trend. Since aggressiveness is normalized by the baselines at each track, the raw percentages between the tracks cannot be compared. From an absolute approach, NCAT is less transient overall, so changes in aggressiveness affect the relative percentages at NCAT more.

The lead truck, A1, drives with same transiency as the leader of the four-truck platoon as it does during undisturbed baseline runs. This finding makes sense since the lead truck's cruise control is barely influenced whether or not subsequent trucks are in its slipstream. Furthermore, both tracks show close to zero aerodynamic benefits for the lead truck. In contrast, the second truck in the configuration, T14, sees 10% energy savings at NCAT and 8% at ACM. However, T14's average $(v \cdot a_{pos})^{95}$ increases compared to baseline runs at both tracks. While the increase in relative percentages at ACM is moderate, it is substantial at NCAT. The increase in transiency has a considerable effect on the third truck, T13. Both at NCAT and ACM, a large increase in relative aggressiveness is observed. While T13 should experience the same aerodynamic benefits as T14, its energy savings are close to zero on both tracks. Comparing these results with Figures 15 and 16 substantiates the suspicion there is a correlation between $(v \cdot a_{pos})^{95}$ and energy savings.

FIGURE 17 Average aggressiveness and energy savings for all trucks in all 100 ft four-truck runs at NCAT

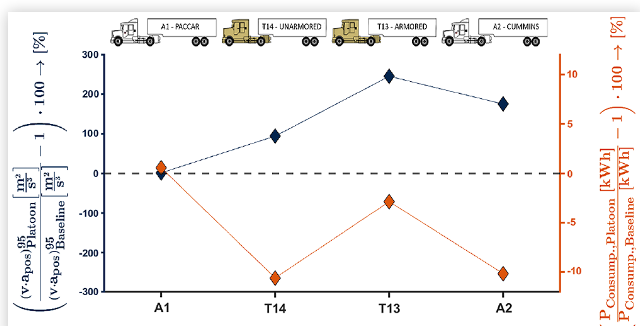

FIGURE 18 Average aggressiveness and energy savings for all trucks in all 100 ft four-truck runs at ACM

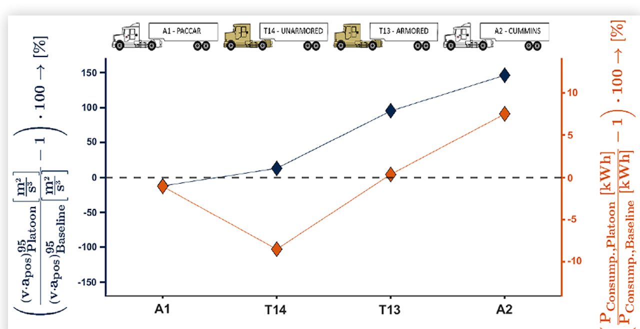

The last truck, A2, sees a change in behavior for the different tracks. While A2 is able to reduce its transiency from that of T13 and therefore retains its energy benefits at NCAT, it is not able to do the same at ACM. In fact, A2 increases its transiency at ACM beyond that of the third truck, T13, resulting in a higher energy usage than during baseline runs. This implies there is a threshold at which the controller is unable to dampen the transiency. While the platoon is below that threshold at NCAT, the transiency is pushed past the threshold at ACM.

The analysis has provided much evidence $(v \cdot a_{pos})^{95}$ is a useful tool when describing platooning dynamics. Additionally, a correlation has been found between $(v \cdot a_{pos})^{95}$ and energy savings. To combine these results, Figures 19 and 20 plot the energy savings directly against the change in transiency during platooning.

Just as in Figures 15 and 16, negative values represent energy savings and less transiency in individual laps, while positive numbers represent increased energy usage and aggressiveness. Both for the following trucks at 100 ft and 50 ft, a trend can be observed between the aggressiveness and the energy savings. While there is insufficient data to claim a sure correlation, the plots suggest a linear correlation exists between aggressiveness and fuel savings of a heavy-duty truck in platooning configurations. If this trend is extrapolated for both the 50- and 100 ft two-truck platoons, best case energy savings appear to be around 8% and 6% respectively for the laps with a similar aggressiveness as baseline runs.

To summarize these findings, Figure 21 shows the same data as previously shown in Figure 15 while excluding individual laps with a 75% or higher increase in transiency compared to their baseline. In doing so, it is implied that controller enhancements improve the ability to follow the lead trucks without excessively increasing aggressiveness. This shifts the maximum of the calculated normalized distribution to −6.2% for 50 ft runs and −3.2% for 100 ft runs. Compared to the prior results of −5.2% and −0.5% when all laps were previously included, realizable energy savings can be seen now for both headways with controller improvements that eliminate laps with the highest levels of enhanced driving aggression.

Conclusions

In conclusion, this study shows RDE metrics can be applied to heavy-duty platooning with minor adjustments to the RDE metrics $(v \cdot a_{pos})^{95}$ and *RPA*. With the adjustments applied, both RDE metrics showed similar trends when evaluating the aggressiveness induced by the platooning controller. Therefore, $(v \cdot a_{pos})^{95}$ was designated the metric of choice.

During periods where CACC operation induced increased aggressiveness, energy savings were lower than expected; and some cases saw negligible energy savings. A correlation between $(v \cdot a_{pos})^{95}$ and energy savings was discovered at NCAT and ACM. The large disparity in acceleration dynamics (due to grade changes) between the tracks increases confidence in the broad applicability of the correlation discovered in this study. Hence, controller enhancements with a focus on

FIGURE 19 Lap-wise aggressiveness against energy savings of the following trucks for all 50 ft two-truck platoons at ACM and NCAT

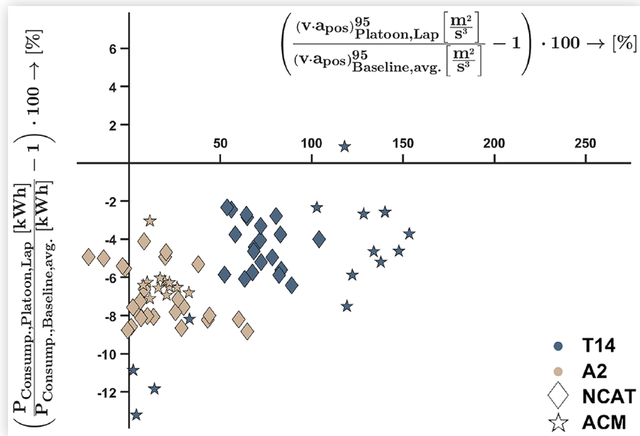

FIGURE 20 Lap-wise aggressiveness against energy savings of the following trucks for all 100 ft two-truck platoons at ACM and NCAT

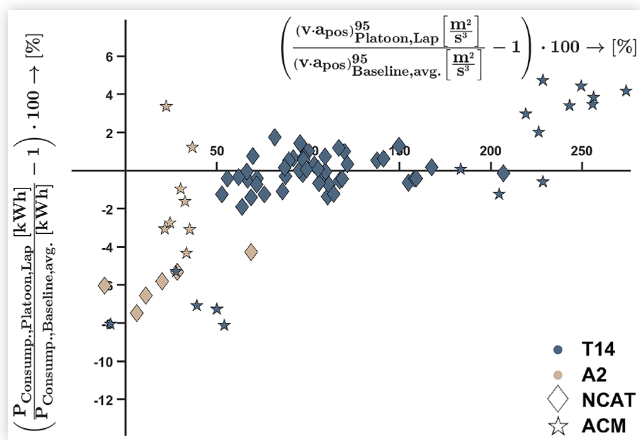

FIGURE 21 Potential overall energy savings per lap for the following trucks in two-truck platoons with only less aggressive laps included

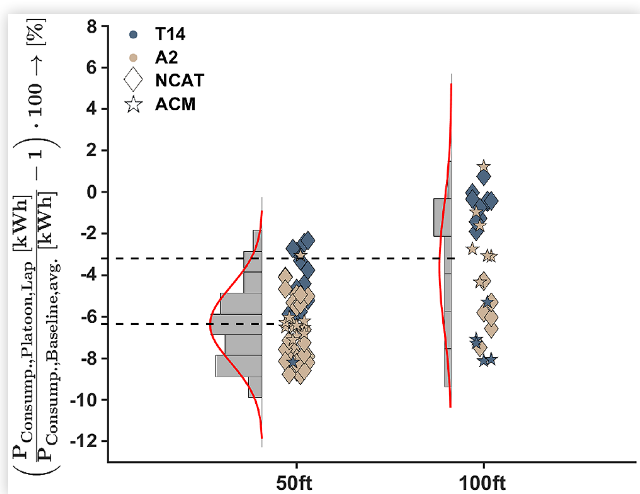

reducing transient behavior should result in energy savings for all cases.

Several assumptions were necessary to complete the analysis herein. The authors acknowledge the imperfect nature of these assumptions, and offer comments regarding future testing campaigns:

1. Corners make up 35% of the track distance at NCAT and could scatter the energy savings results due to changing slipstream conditions.
2. The threshold for positive acceleration was arbitrarily chosen without scientific legitimization. The collecting of more data in future testing campaigns will support or deny the validity of this decision.
3. Lap selection was done on a qualitative basis to distinguish indicative laps for evaluation. Identifying self-similar laps by speed signal resulted in a large number of irregular laps, particularly at ACM. Therefore, future studies should consider alternative approaches to lap selection.
4. Further controller development will improve confidence in the correlation between energy savings and driving aggressiveness.

These suggestions are currently being employed in a fresh testing campaign to further validate the findings from this study.

References

1. Paterlini, G., Yucel, S., MoranLucking, M., and Magnuson, J., "Rolling Resistance Validation - Minnesota Department of Transportation," 2015.
2. United States EPA, "Inventory of U.S. Greenhouse Gas Emissions and Sinks."
3. Roeth, M., "An Analysis of the Operational Costs of Trucking," 2015.
4. Bishop, R., Bevly, D., Humphreys, L., Boyd, S., and Murray, D., "Evaluation and Testing of Driver-Assistive Truck Platooning: Phase 2 Final Results," *Transportation Research Record: Journal of the Transportation Research Board* 2615, 2017, doi:10.3141/2615-02.
5. Roberts, J., Mihelic, R., Roeth, M., and Rondini, D., "Confidence Report on Two-Truck Platooning," 2016.
6. McAuliffe, B., Lammert, M., Lu, X.-Y., Shladover, S. et al. "Influences on Energy Savings of Heavy Trucks Using Cooperative Adaptive Cruise Control," 2018. DOI: 10.4271/2018-01-1181.
7. Ward, J., Smith, P., Pierce, D., Bevly, D. et al., "Cooperative Adaptive Cruise Control (CACC) in Controlled and Real-World Environments: Testing and Results," 2019.
8. Siefert, J., "Creation of an Evaluation Approach for RDE Test Runs on an Engine in the Loop Test Bench," Master's Thesis, Karlsruher Institut für Technologie, 2020.
9. Ellis, M., Gargoloff, J., and Sengupta, R., "Aerodynamic Drag and Engine Cooling Effects on Class 8 Trucks in Platooning Configurations," *SAE Int. J. Commer. Veh.* 8(2), 2015. https://doi.org/10.4271/2015-01-2896.
10. McAuliffe, B., Raeesi, A., Lammert, M., Smith, P. et al., "Impact of Mixed Traffic on the Energy Savings of a Truck Platoon," *WCX SAE World Congress Experience*, 2020, doi:10.4271/2020-01-0679.
11. Lammert, M.P., McAuliffe, B., Smith, P., Raeesi, A. et al., "Impact of Lateral Alignment on the Energy Savings of a Truck Platoon," *WCX SAE World Congress Experience*, 2020, doi:10.4271/2020-01-0594.
12. Bevly, D., Murray, C., Lim, A., Turochy, R., et al., "Heavy Truck Cooperative Adaptive Cruise Control: Evaluation, Testing, and Stakeholder Engagement for Near Term Deployment: Phase One Final Report," 2020.
13. Smith, P. and Bevly, D., "Analysis of On-Road Highway Testing for a Two Truck Cooperative Adaptive Cruise Control (CACC) Platoon," Commercial Vehicle Engineering Congress, 2020, doi:10.4271/2020-01-5009.
14. European Commission, Directorate-General for Internal Market—Industry—Entrepreneurship and SMEs, "Commission Regulation (EU) 2017/1151 of 1 June 2017," 2017.
15. wunderground.com, "Columbus Metropolitan Airport Station," accessed Nov. 20, 2020.
16. wunderground.com, "Willow Run Station," accessed Nov. 20, 2020.

Contact Information

Jan Siefert
Germany
mail@jan-siefert.com

Definitions/Abbreviations

A1 - Peterbilt 579 with Paccar engine
A2 - Peterbilt 579 with Cummins engine
ACC - Adaptive Cruise Control
ACM - American Center for Mobility
CACC - Cooperative Adaptive Cruise Control
CAN - Controller Area Network
DSRC - Dedicated Short Range Communications
EU - European Union
GAVLAB - The GPS and Vehicle Dynamics Laboratory at Auburn University
GPS - Global Positioning System
NCAT - National Center for Asphalt Technology
Φ - Track Position Angle
RDE - Real Driving Emissions
ROS - Robotic Operating Software
RPA - Relative Positive Acceleration
RPM - Revolutions per Minute
T13 - Unarmored Freightliner M915A5
T14 - Armored Freightliner M915A5
V2V - Vehicle to Vehicle
$(v \cdot a_{pos})^{95}$ - 95th Percentile of the $(v \cdot a_{pos})_i$ array

Appendix

TABLE 2 Weather at NCAT during the 2019 testing campaign [15]

Date	T_{max}[°C]	T_{avg}[°C]	T_{min}[°C]	RH_{max}[%]	RH_{avg}[%]	RH_{min}[%]	$v_{wind,max}\left[\frac{m}{s}\right]$	$v_{wind,avg}\left[\frac{m}{s}\right]$	$v_{wind,min}\left[\frac{m}{s}\right]$	Precipitation [mm]
09/16	23	21	19	97	89	71	12	8	6	0
09/19	23	21	19	84	74	66	6	4	0	0
09/20	24	19	16	73	62	46	10	5	3	0
09/23	26	21	18	80	71	56	4	2	0	0
09/24	23	21	19	96	90	76	6	4	2	0
09/25	27	23	20	97	85	64	5	2	0	5.5
09/26	29	22	18	100	78	49	4	1	0	0
09/27	27	24	20	90	80	68	6	3	0	0
10/02	23	18	12	72	49	27	5	3	0	0
10/03	24	17	9	86	58	34	5	2	0	0
10/04	24	18	12	87	64	44	4	2	0	0

TABLE 3 Weather at ACM during the 2019 testing campaign [16]

Date	T_{max}[°C]	T_{avg}[°C]	T_{min}[°C]	RH_{max}[%]	RH_{avg}[%]	RH_{min}[%]	$v_{wind,max}\left[\frac{m}{s}\right]$	$v_{wind,avg}\left[\frac{m}{s}\right]$	$v_{wind,min}\left[\frac{m}{s}\right]$	Precipitation [mm]
10/16	18	11	9	86	74	66	17	11	7	45
10/17	14	9	6	76	64	45	17	11	3	0
10/18	15	7	2	89	70	41	7	3	0	0
10/22	18	13	10	81	69	49	19	11	6	127
10/23	17	11	6	79	57	34	17	9	3	20
10/24	14	11	7	77	60	47	9	5	0	0
10/28	19	10	4	93	78	50	11	4	0	0
10/29	17	11	8	93	82	65	13	5	0	0

ISSN 0148-7191